Physica E 148 (2023) 115624

Contents lists available at ScienceDirect

Physica E: Low-dimensional Systems and Nanostructures

journal homepage: www.elsevier.com/locate/physe

Expansion of nanotube cap due to migration of sp atoms from lateral surface

Yulia G. Polynskaya [a], Alexander S. Sinitsa [b], Sergey A. Vyrko [c], Ottorino Ori [d], Andrey M. Popov [e], Andrey A. Knizhnik [a], Nikolai A. Poklonski [c,*], Yurii E. Lozovik [e]

[a] *Kintech Lab Ltd., 3rd Khoroshevskaya Street 12, Moscow 123298, Russia*
[b] *National Research Centre "Kurchatov Institute", Kurchatov Square 1, Moscow 123182, Russia*
[c] *Physics Department, Belarusian State University, Nezavisimosti Ave. 4, Minsk 220030, Belarus*
[d] *Actinium Chemical Research, 00133 Rome, Italy*
[e] *Institute for Spectroscopy Russian Academy of Science, Fizicheskaya Str. 5, Troitsk Moscow, 108840, Russia*

ARTICLE INFO

Dataset link: https://doi.org/10.17632/trgdpzm3gz

Keywords:
Transformation of sp^2 structure
sp atom
DFT calculations
Nanotube cap
Topological roundness

ABSTRACT

Possible mechanism of cap expansion of preliminarily prepared carbon nanotube is proposed and confirmed by DFT calculations. According to this mechanism single carbon atoms adsorbed on lateral surface of the nanotube (sp atoms) migrate along the nanotube and are trapped at its cap in the potential well. When pair of sp atoms meet at the cap they annihilate with significant energy gain so that expansion of pure sp^2 structure occurs. According to performed calculations on example of (9,0) nanotube the energy gain (or depth of the potential well) with displacement of the first and second sp atom from the lateral surface of nanotube to its cap is of about 1.5 eV. The calculated barriers along these sp-atom displacement paths toward the cap are low and lay in the range 0.25–1.5 eV. The calculated energy gain at the sp-atom pair annihilation is 5–6 eV. The analysis of topological changes at the proposed nanotube cap expansion shows that it leads to the change of the cap structure and therefore to change of the related properties that can be used in applications.

1. Introduction

Advances of modern nanotechnology in last decades lead to elaboration of methods to synthesize new carbon low-dimensional materials such as fullerenes [1], nanotubes [2] and graphene [3]. Treatment of these materials after their synthesis opens up further possibilities for production of new carbon-based systems for nanoscale device design [4]. For example, various methods of a such treatment of preliminary synthesized carbon low-dimensional materials include filling of carbon nanotubes by different materials [5], formation of endohedral fullerenes in a noble-gas atmosphere [6], formation of flat nanotubes from bilayer graphene nanoribbons under electron irradiation [7], formation of hard nanomaterial from fullerite under pressure, preparation of heterostructures consisting of layers of different 2D materials (see, e.g. Ref. [8] for a review) and so on.

Possibility of carbon nanotube growth at a cap with participation of single carbon atoms has been proposed based on the experiment showing the role of single atoms in formation of abundant fullerene isomers [9]. Here we have proposed a method of cap expansion of preliminary synthesized carbon nanotubes with participation of single carbon atoms and study the atomistic mechanism of this process by density functional theory (DFT) calculations. The atomistic mechanism of the proposed process includes three stages: (1) migration of single carbon atoms along a nanotube axis to a nanotube apex, (2) trapping of single carbon atoms in the potential well at a nanotube cap, (3) meeting of two trapped atoms with formation of pure sp^2 structure. The process of nanotube cap expansion proposed here considerably differs from processes at nanotube growth. First, it takes place for preliminarily prepared nanotubes after the nanotube synthesis. Second, whereas a lateral surface of the nanotube with length up to centimeters forms during nanotube growth [10,11] the considered cap expansion retains the lateral surface the same. Third, insertions of only tens atoms can be enough to considerably change the cap structure and related properties. Therefore this process can occur with very low rate of carbon atoms supplied to the nanotube and lower temperature than the nanotube growth.

Migration of single carbon atoms on a lateral surface of a carbon nanotube to the growing end attached to a catalyst nanoparticle has been proposed to play important role in atomistic mechanism of carbon nanotube growth [12–14]. If a source of single carbon atoms to lateral surface of a preliminary synthesized nanotube is available, such atoms can migrate along the lateral surface to the nanotube cap. According to DFT calculations the adsorption energy of a single carbon atom is 1.4 eV [15] and 1.7 eV [16,17] on graphene, corresponds to the

---

* Corresponding author.
E-mail addresses: popov-isan@mail.ru (A.M. Popov), poklonski@bsu.by (N.A. Poklonski).

https://doi.org/10.1016/j.physe.2022.115624
Received 29 July 2022; Received in revised form 17 December 2022; Accepted 19 December 2022

range from 2.0 to 3.3 eV [18] and from 2.5 to 3.5 eV [19] for the ground state position of the sp atom on outer lateral surface of different carbon nanotubes, and is 3 eV [20] and 4.8 eV [21] for C_{61} and C_{59} odd fullerenes, respectively. Moreover DFT calculations show that the adsorption energy of the sp atom decreases with the increase of the nanotube diameter [18,19]. Thus on the average, the adsorption energy for sp carbon atom at sp^2 carbon structure increases with the increase of sp^2 structure curvature. Since sp^2 structure curvature is greater at the nanotube cap than at the lateral surface we propose that if the migrating sp atom reaches the nanotube cap it can be trapped in the potential well. Thus the probability of meeting of two single carbon sp atoms at the cap is considerably greater than at the lateral surface. If two trapped sp atoms meet at the cap they can form pure sp^2 structure due to the reaction of sp-atom pair annihilation [21–24]. This means that the new sp^2 structure forms at the nanotube cap due to the migration of single carbon atoms along the nanotube axis to the apex.

In the present paper we perform DFT study of one step of the cap expansion to prove that proposed atomistic mechanism is energetically favorable. Migration of single carbon sp atom on graphene [15,17,25], lateral surface of carbon nanotubes [18,19] and fullerenes [23] have been studied previously by DFT calculations. Here we apply DFT calculations to study such a migration from a lateral surface to a cap of a carbon nanotube. The analysis of topological changes at the subsequent steps of the proposed cap expansion performed here shows that this expansion leads to the considerable change of the cap structure and therefore to change of the related properties that can be used in applications.

2. Methods

We consider the proposed atomistic mechanism of nanotube cap expansion on example of (9,0) nanotube with the caps that are half of fullerene C_{60} with icosahedral symmetry. Bridge positions (that is instead or above the bond) has been found to correspond to minimal energy of sp carbon atom present in sp^2 carbon structure [16]. Due to high D_{3h} symmetry of the considered capped nanotube the number of nonequivalent bonds of the cap and lateral surface decreases enough to calculate the total energies for all possible nonequivalent single sp-atom positions within DFT approach. The lateral surface of the capped nanotube used in the majority of calculations consists of 4 zigzag rings of atoms and the total number of atoms in the system (except one or two additional sp atoms) is equal to 114 (see Fig. 1a). For example, the difference in the relative energy of the reconstructed zigzag graphene edge with respect to the unreconstructed one between graphene zigzag nanoribbons with 4 and 12 zigzag rows of atoms in width is only 0.05 eV per pentagon–heptagon pair [26]. Thus we believe that 4 zigzag rings of atoms of the lateral surface is sufficient for our qualitative DFT study.

Centimeters long defect-free carbon nanotubes have been synthesized [11]. Thus we have restricted ourselves to the consideration of sp-atom diffusion on perfect nanotube lateral surface. However trapping of single sp atoms in structural defects of nanotube lateral surface is possible. Such trapping of two single sp atoms with subsequent annihilation of sp-atom pair can lead in principle to transformation of sp^2 structure or even to healing of the defect. For example, annihilation of sp-atom pairs is observed at molecular dynamics simulation of healing of a hole in a carbon nanotube under electron irradiation [24]. Here we consider the case of very low concentration of single sp atoms adsorbed on nanotube lateral surface. Consideration of processes at meeting of single sp atoms at nanotube lateral surface is beyond the scope of the present paper.

Structure optimizations were performed with the spin-polarized DFT using PBE functional [27]. The Priroda code [28] was used for the all-electron calculations within the scalar-relativistic approach, which is based on the full four-component one-electron Dirac equation [29] with separation of the spin–orbit effects. The adequacy of Priroda code have been confirmed by comparison of calculated energetic and structural parameters of small metal–oxygen systems [30] and adsorption energy of oxygen on different carbon nanostructures [31] with the results obtained using other DFT-based codes. The energy-optimized extended Gaussian basis set of triple-n quality of the large component and the corresponding kinetically balanced basis for the small component were used [32]. The transition state (TS) structures were determined using the Berni algorithm [33]. To confirm the TS structure, intrinsic reaction coordinate (IRC) calculations [34] were performed by following the single imaginary mode. All energies were calculated taking into account zero point energy.

To find suitable initial guess structure of the transition state (necessary in the IRC method), the structures of the capped nanotube with sp atoms have been optimized using the reactive REBO-1990EVC potential [35] implemented in the in-house MD-kMC code [36]. The parameters of this modified version of the first-generation Brenner potential have been fitted to describe energies of carbon chains, graphene edges, elastic energies of fullerenes, and vacancy migration in graphene, which makes it an adequate choice for study of carbon sp^2 structure. This potential was previously used to study sp-defect migration in an odd fullerene [23]. First, optimization of the capped (9,0) nanotube structures was performed using this empirical potential. Then, the initial guess structure of transition state was found as an output of the reaction path calculation with the nudged elastic band method [37]. This approach allowed us to save the efforts to find the guess structure of transition state, which is crucial for the IRC method.

3. Nanotube cap expansion

3.1. DFT study of one step of cap expansion

We use DFT calculations to consider the following processes at the proposed atomistic mechanism of nanotube cap expansion: (1) migration of the first sp atom from the nanotube lateral surface to the cap, (2) migration of the second sp atom from the nanotube lateral surface to the cap, (3) meeting of two sp atoms at the cap and the annihilation reaction with formation of pure sp^2 structure.

First, we consider the structure and energetics of the capped (9,0) nanotube with one and two additional sp atoms. The structure of the capped (9,0) nanotube has been optimized for all 16 different positions of the single sp atom at the cap and the lateral surface possible for D_{3h} symmetry of the nanotube. The considered positions of sp atom and the calculated total energies relative to the ground state position at the cap with the minimal total energy are presented in Fig. 1a and Table 1, respectively. The adsorption energy of sp atom at the ground state position 6 (see Fig. 1a) is 5.42 eV. This is in a good agreement with the corresponding values 3 eV [20] and 4.8 eV [21] for C_{61} and C_{59} odd fullerenes, respectively.

For 6 of the considered positions of the sp atom there is a chemical bond under the sp atom with the length from 1.49 to 1.68 Å (these positions are indicated by " + " in Table 1). The other 10 positions of the sp atom are without the bond under the sp atom with the distance between neighboring atoms of the sp atom from 2.12 to 2.24 Å. Thus we do not use here the term adatom for general case of the sp atom present in the nanotube structure. Previously isomers with and without a bond under a sp atom have been found for odd fullerene C_{61} [38]. The total energy of the nanotube with different positions of the sp atom at the cap is 1.0–1.6 eV lower than the total energy of the nanotube with the sp atom located at the lateral surface. This means that the single sp atom can be trapped in the potential well at the nanotube cap.

For the consideration of the nanotube with two additional sp atoms the position of the first sp atom has been chosen to correspond to the minimal total energy of the nanotube with the single sp atom (this position is indicated by letter A in Fig. 1c). 15 different positions of the second sp atom nearby the first sp atom have been considered. 7

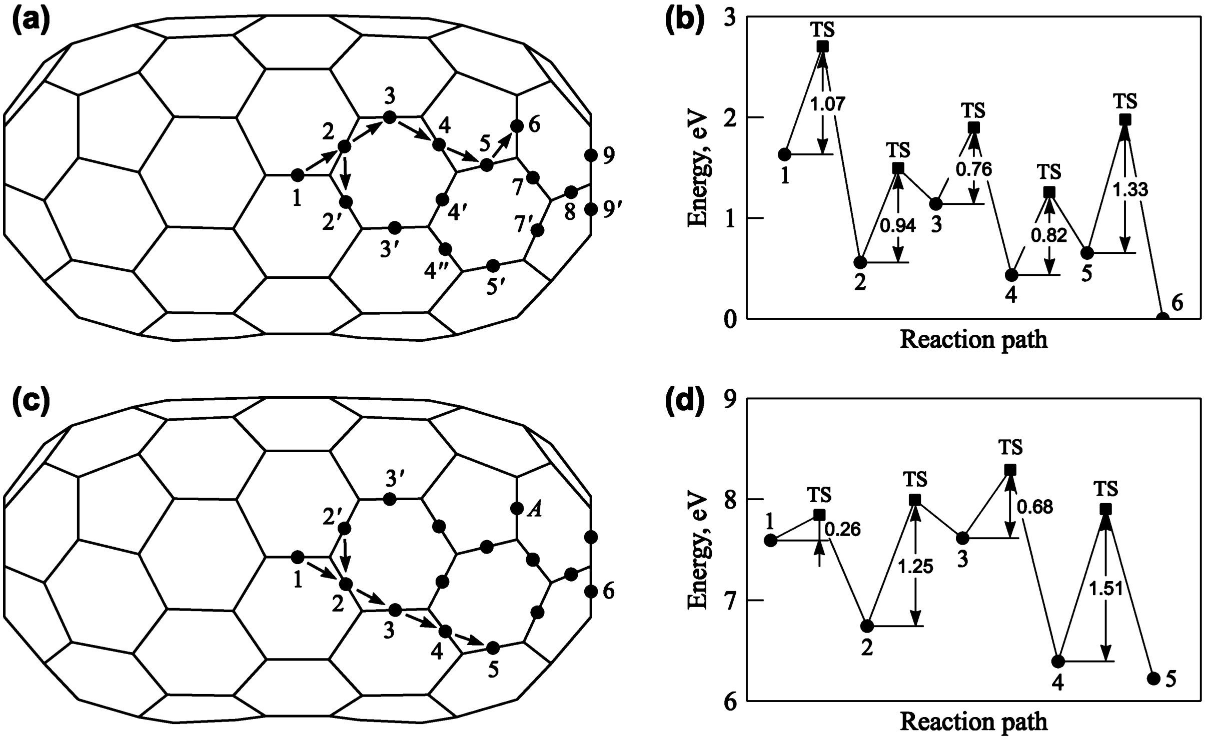

Fig. 1. Left panels: The structure of the capped (9,0) nanotube used in the DFT calculations with considered positions of sp atoms instead or above the bond. The subsequent steps of the considered sp-atom migration paths from the lateral surface to the cap are shown by blue arrows. The considered steps of sp-atom migration along a circumference of the nanotube are shown by green arrows. (a) Single sp atom is present in the nanotube structure. (c) Two sp atoms are present in the nanotube structure. The position of the first sp atom is indicated by *A*. The considered positions of the second sp atom are shown by red and black circles where stable structures with presence of two sp atoms have been found and have not been found, respectively (see text). Right panels: Energetics of the first (b) and second (d) sp-atom migration from the lateral surface to the cap corresponding to paths shown in panels (a) and (c), respectively. The total energies of the optimized structures and of transition states (TS) are shown by filled red circles and by red squares, respectively. Total energy is measured relative to the minimal energy (ground state isomer with the single sp atom and nanotube with pure sp^2 structure shown in Fig. 2b for nanotubes with presence of one and two sp atoms, respectively). The activation barriers of the sp-atom migration are indicated.

out of 15 considered positions where the second sp atom is close to the first sp atom are found to be unstable with formation of pure sp^2 structure and cannot occur during considered cap expansion whereas other 8 considered structures are stable in presence of two sp atoms (see Fig. 1c and Table 1). The bond under the first sp atom is absent for all 8 stable structures with the distance between atoms neighboring with this sp atom from 2.17 to 2.29 Å. The bond under the second sp atom is present for 3 out of 8 positions of this sp atom with the length from 1.50 to 1.59 Å (see Table 1). For optimized structures without the bond under the second sp atom the distance between neighboring atoms of this sp atom is from 2.12 to 2.26 Å. Total energies averaged over the positions without a bond under the sp atom are lower by 0.62 eV and 1.06 eV than the energies averaged over the positions with a bond under the sp atom for the cases where one and two sp atoms are present in the nanotube sp^2 structure, respectively. Analogously to the case of the single sp atom the total energy of the nanotube decreases by 1.2–1.8 eV with displacement of the second sp atom from the lateral surface to the cap. Therefore the second sp-atom migration from the lateral surface of the nanotube to the cap also can lead to trapping of this sp atom in the potential well at the cap.

Table 1

Calculated relative total energies *E* and bond lengths *b* between atoms neighboring with sp atom for the considered capped (9,0) nanotube with presence of sp atoms in the structure. Total energy for nanotubes with single sp atom is measured relative to the minimal energy calculated for such nanotubes. Total energy for nanotubes with two sp atoms is measured relative to the energy of the nanotube with pure sp^2 structure shown in Fig. 2b. "No." is the number of sp atom indicated in Fig. 1. The cases where the bond is present and absent under the sp atom in the optimized structure are indicated by + and −, respectively.

No.	*E* (eV)	*b* (Å)	Bond	No.	*E* (eV)	*b* (Å)	Bond
Fig. 1a, single sp atom is present							
1	1.63	1.52	+				
2	0.56	2.14	−	2′	0.60	2.16	−
3	1.14	1.49	+	3′	1.54	1.66	+
4	0.43	2.15	−	4′	0.68	1.68	+
5	0.65	2.12	−	5′	0.31	2.23	−
6	0	2.20	−				
7	0.62	1.57	+	7′	0.26	2.17	−
8	0.09	2.20	−				
9	0.36	1.65	+	9′	0.24	2.17	−
				4″	0.60	2.24	−
Fig. 1c, two sp atoms are present							
1-*A*	7.59	1.52	+				
2-*A*	6.74	2.12	−	2′-*A*	6.61	2.14	−
3-*A*	7.62	1.59	+	3′-*A*	7.07	1.50	+
4-*A*	6.39	2.23	−				
5-*A*	6.22	2.26	−				
6-*A*	5.84	2.25	−				

Second, barriers of sp-atom migration from the nanotube lateral surface to the cap have been calculated. The steps of migration path of the first and second sp atoms on the nanotube structure and the calculated barriers are shown in Fig. 1. These barriers are found to be in the range from 0.76 to 1.33 eV and from 0.26 to 1.51 eV for migration of the first and second sp atoms, respectively, from the nanotube lateral surface to the cap. The first step of the considered migration path between sp atom positions 1 and 2 (see Fig. 1) corresponds to the lateral surface of the nanotube. The calculated barrier of migration of single sp atom is 1.07 eV that coincides with the barrier about 1 eV for the migration along the nanotube axis obtained by DFT calculations for the same (9,0) nanotube without a cap [19]. Note that DFT calculations give even the smaller barrier of 0.4 eV for migration of sp atom along the axis of (5,5) armchair nanotube [18]. Thus the obtained barriers for migration from the lateral surface to the cap correspond to the same

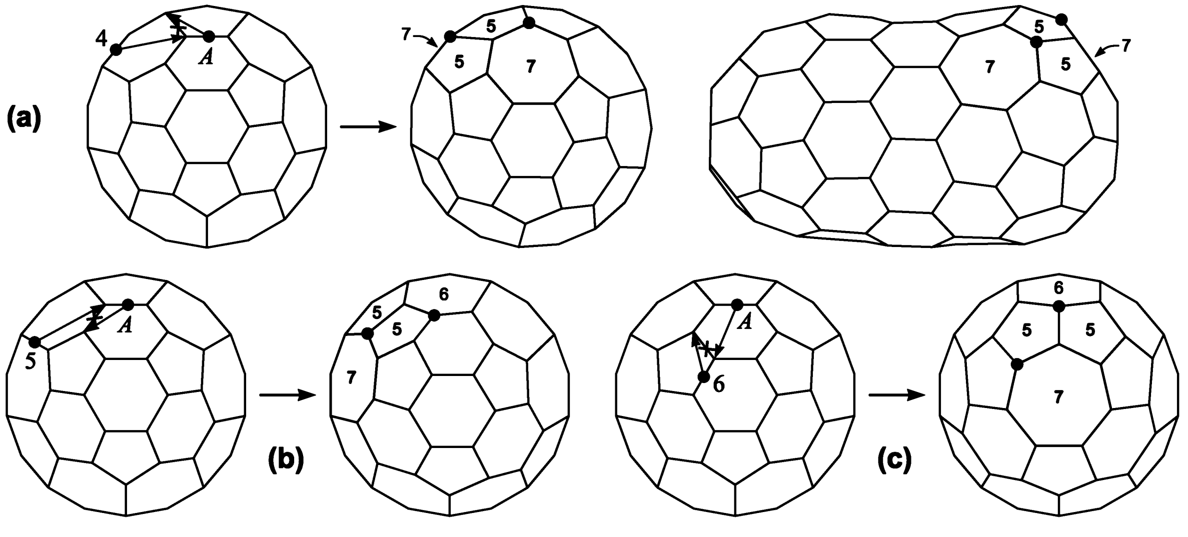

Fig. 2. Schemes of the considered reactions of sp-atom pair annihilation; sp atoms are shown by red circles. The positions of the first and second sp atoms are indicated in the same way as in Fig. 1c. The pentagons and hexagons of the initial structure of the cap are colored in light green and white, respectively. The pentagons, hexagons and heptagons formed during the cap expansion are colored in light red, light yellow and light blue, respectively. Broken bonds are indicated by green crosses. Forming bonds are shown by blue arrows. Formed bonds are shown by red lines.

Table 2
Reaction type (see Fig. 3) and calculated characteristics of the considered in Fig. 2 reactions of sp-atom pair annihilation: energy gain ΔE at the reaction, total energies E relative to the minimal energy after the reaction, topological efficiency ρ_1 and roundness ρ_2 after the reaction, respectively.

	Reaction type	ΔE (eV)	E (eV)	ρ_1	ρ_2
Fig. 2a	6-6-6 → 7-5/5-7	5.08	1.30	1.1916	1.3396
Fig. 2b	6-6-5 → 7-5/5-6	6.22	0	1.1681	1.3148
Fig. 2c	6-6-5 → 7-5/5-6	5.75	0.09	1.2115	1.3464

range as the barriers for migration along axis of zigzag and armchair nanotubes. Barriers for migration along axis of chiral nanotubes should also correspond to this range. According to calculations the barriers for migration along axis of zigzag and armchair nanotubes decrease with increase of the nanotube diameter [19]. Thus there are good reasons to believe that barriers for migration of single carbon atoms from lateral surface to a cap are also low for nanotubes with different chiralities and greater diameters. Therefore the migration of sp atom to a nanotube cap can occur at experimental conditions as observed for the migration along the axis [13,14]. The barriers for migration of sp atom along a circumference of the nanotube have been calculated to be 1.63 and 1.39 eV for the single sp atom and the second sp atom where the first sp atom is located at position A, respectively (the migration steps are shown in Fig. 1a and c for the single and second sp atoms, respectively).

The schemes of considered reactions of sp-atom pair annihilation are shown in Fig. 2. Previously such type of bond rearrangements of carbon network has been found in molecular dynamics simulation for a carbon nanotube [22] and fullerenes [23] and considered for fullerenes using DFT calculations [21]. Here we present schemes of reactions of sp-atom pair annihilation according to [21,23] (scheme presented in [22] has unstable structure before the reaction). The calculated energy gain at the reaction and the total energies after the reaction are presented in Table 2. The calculated energy gain is in agreement with the energy gain 6.23 eV obtained by DFT calculation for sp-atom pair annihilation in C_{70} fullerene [21]. Structural rearrangements with formation of pure sp^2 carbon structure for a case where two sp atoms are initially present in the system have been studied also using tight-binding potential for graphene and lateral surface of (5,5) nanotube on example of merging of two monovacancies with formation of divacancy [39]. The calculated total energy gain at this merging has been found to be about 6 eV that is also in excellent agreement with calculations here. Such a huge energy gain means that there is no question that the pair sp-atom annihilation reaction occurs when two sp atoms meet at the nanotube cap. Note that the nanotube isomers with one heptagon in the structure after the reaction (Fig. 2d and c) have the total energy which is lower by 1.2–1.3 eV than that of isomers with two heptagons in the structure (Fig. 2a).

Let us estimate the minimal temperature which is acceptable for experimental realization of the nanotube cap expansion. Dozens of reactions of sp-atom pair annihilation are enough for considerable change of the cap structure and related properties. We estimate the smallest acceptable rate of single carbon sp atom arrival to the cap as one atom per time $t = 10^3$ s and the average traveled distance for this atom along the nanotube axis $d = 100$ nm. For jump diffusion of the sp atom on the nanotube lateral surface $d^2 = \nu a^2 t/n$, where $\nu = \nu_0 \exp(-E_\mathrm{b}/k_\mathrm{B}T)$ is the jump frequency, ν_0 is the pre-exponential factor, E_b is the barrier to jump on an neighboring adsorption position, T is the absolute temperature, a is the jump length equal to half of the lattice constant of graphene, and $n = 4$ is the number of bonds neighboring with the sp atom. Taking the barrier to jump $E_\mathrm{b} = 1$ eV estimated on the base of the performed DFT calculations and the pre-exponential factor $\nu_0 = 10^{12}$ s^{-1} (see, for example, calculated pre-exponential factor for rotation of bond in Stone–Wales defect of graphene [40]) we have estimated the minimal acceptable temperature of the nanotube cap expansion to be about 600 K.

3.2. Topological analysis of subsequent steps of cap expansion

Let us now discuss the structure of the cap which arises during subsequent steps of the considered mechanism of the cap expansion. The simplest isomerization reaction which changes the polygon positions (thus changes the topology of pure sp^2 structure) is the Stone–Wales pyracylene transformation (SW reaction) [41]. However SW reaction occurs with breaking of two bonds and therefore has considerable activation barrier (contrary to reaction of sp-atom pair annihilation which occurs with breaking of one bond, see Figs. 2 and 3). According to DFT calculations, the value of this barrier is from 4.7 to 7.5 eV for various fullerenes [9,20,21,42–46]. Since the sp^2 structure of the nanotube cap is analogous to that of fullerenes the activation barrier of SW reaction at the nanotube cap should has the high value too. The barrier of SW reaction (all the more the barrier of any complex isomerization reactions) is several times greater than the calculated trapping energy at the nanotube cap, about 1.5 eV, and barriers of sp-atom

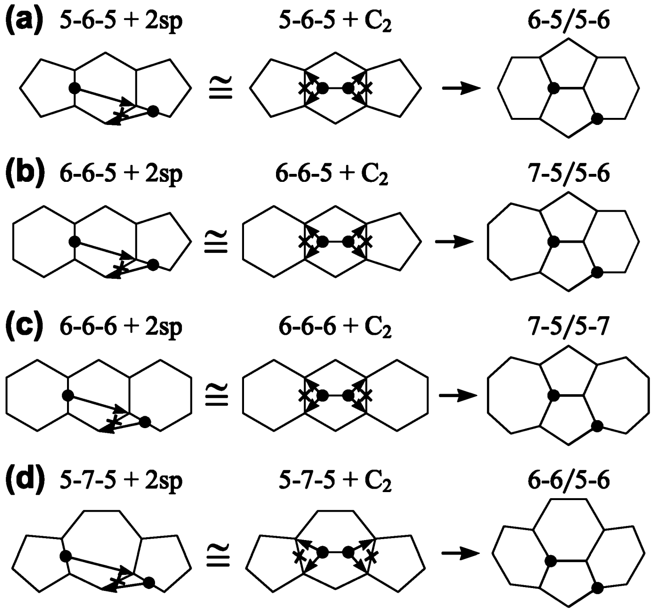

Fig. 3. Schemes of sp^2-structure expansion which show the equivalence of topological changes at annihilation of two sp atoms and Endo–Kroto C_2 molecule insertion on examples of (a) 5-6-5 → 6-5/5-6, (b) 6-6-5 → 7-5/5-6, (c) 6-6-6 → 7-5/5-7, and (d) 5-7-5 → 6-6/5-6 reactions. sp atoms are shown by red circles. The pentagons and hexagons of the initial structure of the cap are colored in light green and white, respectively. The pentagons, hexagons and heptagons formed during the expansion are colored in light red, light yellow and light blue, respectively. Broken bonds are indicated by green crosses. Forming bonds are shown by blue arrows. Formed bonds are shown by red lines.

migration, 0.25–1.5 eV. Thus isomerization reactions are not possible at temperature estimated above where the nanotube cap expansion due to the considered mechanism can occur. Therefore we consider the cap expansion taking into account only topological changes due to the sp atom pair annihilation.

Topological change of sp^2 structure at reaction of sp-atom pair annihilation is equivalent to topological change at Endo–Kroto reaction [47] of C_2 molecule insertion into sp^2 structure. This statement is clearly shown by examples on several identical sets of adjacent polygons involved in both reactions (see Fig. 3). Thus we use in the topological analysis here Endo–Kroto insertion instead of the sp atom pair annihilation.

To predict a new sp^2 structure which arises at the nanotube apex due to the proposed atomistic mechanism of the cap expansion is a task similar to solve the mystery of abundant fullerene isomers formation (like C_{60}-I_h and C_{70}-D_{5h}) and even more difficult challenge since we do not know a final structure. Kinetic models taking into account relation between topological change and probability of reaction can be useful (see Ref. [48] for review on fullerene formation atomistic simulations). Such probabilities can be determined on the base of topological efficiency ρ_1 and topological roundness ρ_2 [49]. Both ρ_1 and ρ_2 have been shown to have a good correlation with the energies of fullerenes and PAH molecules obtained by DFT calculations [50–52] (note that the lower limit by definition $\rho_1, \rho_2 = 1$ for a fullerene C_{60}-I_h). Here the topological efficiency ρ_1 and roundness ρ_2 have been calculated for all three nanotube isomers obtained after the pair sp-atom annihilation reaction (see Fig. 2) using the graph included the cap and the first polygon ring of the lateral surface adjacent to the cap (this ring is different for the isomer shown in Fig. 2a by presence of a heptagon). The minimal values of ρ_1 and ρ_2 corresponds to the nanotube isomer with the minimal energy E (see Table 2). Thus we confirm the conclusion in works [50–52] on correlation between ρ_1 and ρ_2 and the energy of carbon sp^2 structure. Consideration of subsequent steps of the cap expansion by kinetic models is beyond the framework of the present paper.

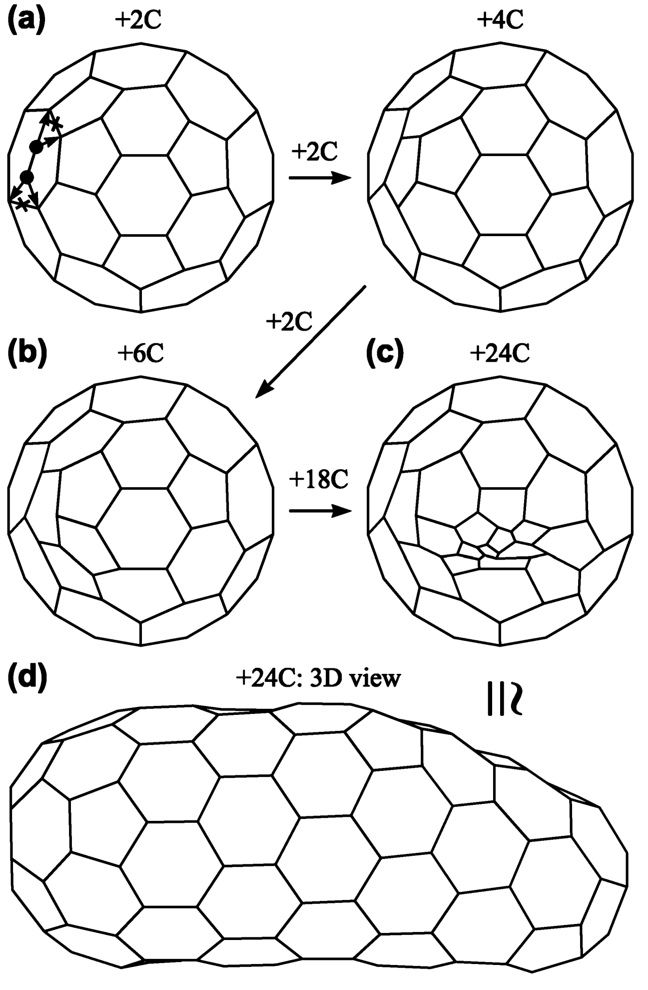

Fig. 4. (a-c) Schemes of cap expansion of the considered capped (9,0) nanotube by subsequent C_2 molecule insertions (this reaction gives the change of topology which is equivalent to sp-atom pair annihilation, see Fig. 3) which continue the first expansion step shown in Fig. 2b. (a) C_2 molecule insertion at the second expansion step. Broken bonds are indicated by green crosses. Forming bonds are shown by blue arrows. (b) Scheme of the cap after the third expansion step. (c) Scheme of the cap after the 12-th expansion step. This is the deadend for C_2 molecule insertion through 5-6-5 units (there are no more pentagons separated by single hexagon). (d) Calculated structure of the nanotube corresponding to the scheme shown in panel (c). Number of carbon atoms inserted into the initial structure of the cap is indicated. The pentagons and hexagons of the initial structure of the cap are colored in light green and white, respectively. The pentagons, hexagons and heptagon formed during the expansion are colored in light red, light yellow and light blue, respectively. Bonds formed during the expansion are shown by red lines.

However we obtain some qualitative conclusions using the simplest model based on assumption that a cap structure without heptagons has some preference analogously to absence of heptagons in sp^2 structure of abundant fullerene isomers [53]. Further steps of the nanotube cap expansion by sp-atom pair annihilation have been considered using this model for two examples of cap structures with one heptagon shown in Fig. 2b and c. The second step of the cap expansion occurs in our consideration by 5-7-5 → 6-6/5-6 reaction to exclude the heptagon from the structure (see Fig. 4a). Then only 5-6-5 → 6-5/5-6 reactions were taking into account (the third step by this reaction is shown in Fig. 4b). We reach the conclusion that for both considered cases such a cap expansion terminates by deadend where further expansion by 5-6-5 → 6-5/5-6 reactions is not possible due to absence of 5-6-5 units in the structure. Several expansion paths with different structures at the deadend are possible, see example shown in Fig. 4c. We believe that this conclusion can be valid not only for the expansion starting from the considered cap structures but also for a general case. Namely, that infinite carbon nanotube cap expansion due to proposed atomistic mechanism by only 5-6-5 → 6-5/5-6 reactions without heptagon formation is not possible. This problem will be considered elsewhere. Probably that caps without heptagons mainly form at standard carbon nanotube production analogously to formation of abundant fullerene isomers without heptagons in the structure. Then conclusion above on necessity of heptagon formation means the change of nanotube apex structure and related properties.

4. Conclusions and discussion

Here we propose atomistic mechanism of cap expansion of preliminary synthesized carbon nanotubes with participation of single carbon sp atoms adsorbed on the nanotube lateral surface. First, the DFT study performed here shows that adsorption energies of single carbon sp atoms for positions at the nanotube cap are by 1–1.5 eV greater than for positions at the lateral surface. This means that such atoms can be trapped at the cap in the potential well. Second, DFT calculations performed give small barriers in the range 0.25–1.5 eV for migration of the sp atom from the lateral surface to the cap of the nanotube whereas analogously small barriers in the range 0.4–1 eV [18,19] have been obtained by previous DFT calculations for migration of the sp atom along the nanotube axis far from the nanotube apex. Therefore single carbon sp atoms supplied on the lateral surface can easily migrate to potential well at the cap at experimental conditions. New sp^2 structure forms at the cap from supplied sp atoms due to the reaction of sp-atom pair annihilation [21–23] with the huge energy gain calculated here to be 5–6 eV.

It is evident that new sp^2 structure arising at the nanotube apex during the cap expansion due to the sp atom pair annihilation is determined by the rate of carbon atoms supplied on the lateral nanotube surface and temperature. At lower rate of supplied atoms and temperature the most energetically favorable position of sp atom pair annihilation at the nanotube cap can be realized. Contrary, for higher rate of supplied atoms and temperature, sp atom pair annihilation can occur at random position at the cap. Thus these parameters can be used to control the new sp^2 structure arising at the nanotube apex.

Careful consideration of the new sp^2 structure arising at the nanotube apex during subsequent steps of cap expansion by the proposed atomistic mechanism is beyond the framework of the present paper. The simplest topological analysis based on assumption the reactions of sp-atom pair annihilation without heptagon formation have preference leads to conclusion that expansion without heptagons is not possible. That is the cap structure cannot be reproduced during the expansion. Moreover the proposed nanotube cap expansion is not bound to occur with conservation of nanotube diameter contrary to growth of a carbon nanotube with diameter determined by a catalyst. In a general way, energy of sp^2 carbon structure decreases with decrease of the curvature. This statement has been shown by DFT calculations both for closed fullerenes [54] and cylindrical nanotubes [55,56]. Thus formation of ball-shaped structure at the nanotube apex analogously to formation of a soap bubble at a straw apex is energetically favorable during the proposed cap expansion.

Carbon nanotubes have shown applications such as scanning probes [57,58] and field emitters [59–61] where operational characteristics determined by the nanotube apex structure. Since the proposed cap expansion of the preliminary synthesized nanotube occurs with considerable change of sp^2 structure at the apex of the nanotube it should lead to change of nanotube properties related with the apex structure and in turn can lead to improvement of operational characteristics of nanotube-based scanning probes and field emitters.

To realize the proposed carbon nanotube cap expansion a source with controllable rate of single carbon atoms should be placed near the preliminary synthesized nanotube. The ejection of single carbon atoms from various carbon-based materials by electron impacts in transmission electron microscope has been observed in a lot of experiments (see Ref. [62] for a review). Thus transmission electron microscope can be used as a source of carbon atoms where rate of supplied atoms can be determined by the electron flux and distance between carbon-based material where ejection of the atoms occurs and the carbon nanotube.

Declaration of competing interest

The authors declare that they have no known competing financial interests or personal relationships that could have appeared to influence the work reported in this paper.

Data availability

The raw data that support the findings of this study are openly available in Mendeley Data at https://doi.org/10.17632/trgdpzm3gz, see Ref. [63].

Acknowledgments

Y.G.P, A.S.S, A.M.P., and Y.E.L. acknowledge support by the Russian Foundation for Basic Research (Grant No. 20-52-00035). S.A.V. and N.A.P. acknowledge support by the Belarusian Republican Foundation for Fundamental Research (Grant No. F23RNF-049) and by the Belarusian National Research Program “Convergence-2025”. O.O. is grateful to Prof. Franco Cataldo at Actinium Rome and Prof. Mihai V. Putz at West University of Timisoara for helpful discussions.

References

[1] H.W. Kroto, J.R. Heath, S.C. O'Brien, R.F. Curl, R.E. Smalley, C_{60}: Buckminsterfullerene, Nature 318 (1985) 162–163, http://dx.doi.org/10.1038/318162a0.

[2] S. Iijima, Helical microtubules of graphitic carbon, Nature 354 (1991) 56–58, http://dx.doi.org/10.1038/354056a0.

[3] K.S. Novoselov, A.K. Geim, S.V. Morozov, D. Jiang, Y. Zhang, S.V. Dubonos, I.V. Grigorieva, A.A. Firsov, Electric field effect in atomically thin carbon films, Science 306 (2004) 666–669, http://dx.doi.org/10.1126/science.1102896.

[4] N.A. Poklonski, S.A. Vyrko, A.I. Siahlo, O.N. Poklonskaya, S.V. Ratkevich, N.N. Hieu, A.A. Kocherzhenko, Synergy of physical properties of low-dimensional carbon-based systems for nanoscale device design, Mater. Res. Express 6 (2019) 042002, http://dx.doi.org/10.1088/2053-1591/aafb1c.

[5] P.M. Ajayan, S. Iijima, Capillarity-induced filling of carbon nanotubes, Nature 361 (1993) 333–334, http://dx.doi.org/10.1038/361333a0.

[6] M. Saunders, H.A. Jiménez-Vázquez, R.J. Cross, R.J. Poreda, Stable compounds of helium and neon: He@C_{60} and Ne@C_{60}, Science 259 (1993) 1428–1430, http://dx.doi.org/10.1126/science.259.5100.1428.

[7] B. Song, G.F. Schneider, Q. Xu, G. Pandraud, C. Dekker, H. Zandbergen, Atomic-scale electron-beam sculpting of near-defect-free graphene nanostructures, Nano Lett. 11 (2011) 2247–2250, http://dx.doi.org/10.1021/nl200369r.

[8] A.K. Geim, I.V. Grigorieva, Van der Waals heterostructures, Nature 499 (2013) 419–425, http://dx.doi.org/10.1038/nature12385.

[9] P.W. Dunk, N.K. Kaiser, C.L. Hendrickson, J.P. Quinn, C.P. Ewels, Y. Nakanishi, Y. Sasaki, H. Shinohara, A.G. Marshall, H.W. Kroto, Closed network growth of fullerenes, Nature Commun. 3 (2012) 855, http://dx.doi.org/10.1038/ncomms185324.

[10] X. Yu, J. Zhang, W. Choi, J.-Y. Choi, J.M. Kim, L. Gan, Z. Liu, Cap formation engineering: From opened C_{60} to single-walled carbon nanotubes, Nano Lett. 10 (2010) 3343–3349, http://dx.doi.org/10.1021/nl1010178.

[11] R. Zhang, Y. Zhang, F. Wei, Controlled synthesis of ultralong carbon nanotubes with perfect structures and extraordinary properties, Acc. Chem. Res. 50 (2017) 179–189, http://dx.doi.org/10.1021/acs.accounts.6b00430.

[12] Y.H. Lee, S.G. Kim, D. Tománek, Catalytic growth of single-wall carbon nanotubes: An *ab initio* study, Phys. Rev. Lett. 78 (1997) 2393–2396, http://dx.doi.org/10.1103/physrevlett.78.2393.

[13] O.A. Louchev, Y. Sato, H. Kanda, Growth mechanism of carbon nanotube forests by chemical vapor deposition, Appl. Phys. Lett. 80 (2002) 2752–2754, http://dx.doi.org/10.1063/1.1468266.

[14] D.-H. Kim, H.-S. Jang, C.-D. Kim, D.-S. Cho, H.-S. Yang, H.-D. Kang, B.-K. Min, H.-R. Lee, Dynamic growth rate behavior of a carbon nanotube forest characterized by in situ optical growth monitoring, Nano Lett. 3 (2003) 863–865, http://dx.doi.org/10.1021/nl034212g.

[15] P.O. Lehtinen, A.S. Foster, A. Ayuela, A. Krasheninnikov, K. Nordlund, R.M. Nieminen, Magnetic properties and diffusion of adatoms on a graphene sheet, Phys. Rev. Lett. 91 (2003) 017202, http://dx.doi.org/10.1103/PhysRevLett.91.017202.

[16] L. Li, S. Reich, J. Robertson, Defect energies of graphite: Density-functional calculations, Phys. Rev. B 72 (2005) 184109, http://dx.doi.org/10.1103/PhysRevB.72.184109.

[17] V.O. Özçelik, H.H. Gurel, S. Ciraci, Self-healing of vacancy defects in single-layer graphene and silicene, Phys. Rev. B 88 (2013) 045440, http://dx.doi.org/10.1103/PhysRevB.88.045440.

[18] L. Han, P. Krstic, I. Kaganovich, R. Car, Migration of a carbon adatom on a charged single-walled carbon nanotube, Carbon 116 (2017) 174–180, http://dx.doi.org/10.1016/j.carbon.2017.02.003.

[19] A.V. Krasheninnikov, K. Nordlund, P.O. Lehtinen, A.S. Foster, A. Ayuela, R.M. Nieminen, Adsorption and migration of carbon adatoms on carbon nanotubes: Density-functional *ab initio* and tight-binding studies, Phys. Rev. B 69 (2004) 073402, http://dx.doi.org/10.1103/PhysRevB.69.073402.

[20] B.R. Eggen, M.I. Heggie, G. Jungnickel, C.D. Latham, R. Jones, P.R. Briddon, Autocatalysis during fullerene growth, Science 272 (1996) 87–89, http://dx.doi.org/10.1126/science.272.5258.87.

[21] W.-W. Wang, J.-S. Dang, X. Zhao, S. Nagase, Revisit of the Saito–Dresselhaus–Dresselhaus C_2 ingestion model: on the mechanism of atomic-carbon-participated fullerene growth, Nanoscale 9 (2017) 16742–16748, http://dx.doi.org/10.1039/C7NR04966H.

[22] A. Maiti, C.J. Brabec, J. Bernholc, Kinetics of metal-catalyzed growth of single-walled carbon nanotubes, Phys. Rev. B 55 (1997) R6097–R6100, http://dx.doi.org/10.1103/PhysRevB.55.R6097.

[23] A.S. Sinitsa, I.V. Lebedeva, Y.G. Polynskaya, A.M. Popov, A.A. Knizhnik, Molecular dynamics study of sp-defect migration in odd fullerene: possible role in synthesis of abundant isomers of fullerenes, J. Phys. Chem. C 124 (2020) 11652–11661, http://dx.doi.org/10.1021/acs.jpcc.0c00650.

[24] I.V. Lebedeva, A.M. Popov, A.A. Knizhnik, Healing of a hole in a carbon nanotube under electron irradiation in high-resolution transmission electron microscopy, J. Phys. Chem. C 125 (2021) 1523–1530, http://dx.doi.org/10.1021/acs.jpcc.0c09326.

[25] M.T. Lusk, L.D. Carr, Nanoengineering defect structures on graphene, Phys. Rev. Lett. 100 (2008) 175503, http://dx.doi.org/10.1103/PhysRevLett.100.175503.

[26] Y.G. Polynskaya, I.V. Lebedeva, A.A. Knizhnik, A.M. Popov, Optimal model of semi-infinite graphene for *ab initio* calculations of reactions at graphene edges by the example of zigzag edge reconstruction, Comput. Theor. Chem. 1214 (2022) 113755, http://dx.doi.org/10.1016/j.comptc.2022.113755.

[27] J.P. Perdew, K. Burke, M. Ernzerhof, Generalized gradient approximation made simple, Phys. Rev. Lett. 77 (1996) 3865–3868, http://dx.doi.org/10.1103/PhysRevLett.77.3865.

[28] D.N. Laikov, Y.A. Ustynyuk, PRIRODA-04: a quantum chemical program suite. New possibilities in the study of molecular systems with the application of parallel computing, Russ. Chem. Bull. Int. Ed. 54 (2013) 820–826, http://dx.doi.org/10.1007/s11172-005-0329-x.

[29] K.G. Dyall, An exact separation of the spin-free and spin-dependent terms of the Dirac–Coulomb–Breit Hamiltonian, J. Chem. Phys. 100 (1994) 2118–2127, http://dx.doi.org/10.1063/1.466508.

[30] D.A. Pichugina, Y.G. Polynskaya, N.E. Kuz'menko, Spin and structural features of oxygen dissociation on tetrahedral Ag_{20} and $Ag_{19}Au$ clusters, Phys. Chem. Chem. Phys. 18 (2016) 18033–18044, http://dx.doi.org/10.1039/c6cp01630h.

[31] Y.G. Polynskaya, N.A. Matsokin, A.S. Sinitsa, A.A. Knizhnik, B.V. Potapkin, First-principles investigation of interaction between the atomic oxygen species and carbon nanostructures, Carbon Trends 9 (2022) 100201, http://dx.doi.org/10.1016/j.cartre.2022.100201.

[32] D.N. Laikov, A new class of atomic basis functions for accurate electronic structure calculations of molecules, Chem. Phys. Lett. 416 (2005) 116–120, http://dx.doi.org/10.1016/j.cplett.2005.09.046.

[33] H.B. Schlegel, Optimization of equilibrium geometries and transition structures, J. Comput. Chem. 3 (1982) 214–218, http://dx.doi.org/10.1002/jcc.540030212.

[34] C. Gonzalez, H.B. Schlegel, An improved algorithm for reaction path following, J. Chem. Phys. 90 (1989) 2154–2161, http://dx.doi.org/10.1063/1.456010.

[35] A.S. Sinitsa, I.V. Lebedeva, A.M. Popov, A.A. Knizhnik, Long triple carbon chains formation by heat treatment of graphene nanoribbon: molecular dynamics study with revised Brenner potential, Carbon 140 (2018) 543–556, http://dx.doi.org/10.1016/j.carbon.2018.08.022.

[36] A.A. Knizhnik, MD-kMC Code, Kintech Lab Ltd., Moscow, 2006–2018.

[37] G. Henkelman, H. Jónsson, Improved tangent estimate in the nudged elastic band method for finding minimum energy paths and saddle points, J. Chem. Phys. 113 (2000) 9978–9985, http://dx.doi.org/10.1063/1.1323224.

[38] L. Tsetseris, S.T. Pantelides, Intermolecular bridges and carrier traps in defective C_{60} crystals, Phys. Rev. B 84 (2011) 195202, http://dx.doi.org/10.1103/PhysRevB.84.195202.

[39] A.T. Lee, B. Ryu, I.-H. Lee, K.J. Chang, Action-derived molecular dynamics simulations for the migration and coalescence of vacancies in graphene and carbon nanotubes, J. Phys.: Condens. Matter 26 (2014) 115303, http://dx.doi.org/10.1088/0953-8984/26/11/115303.

[40] J. Ma, D. Alfè, A. Michaelides, E. Wang, Stone-Wales defects in graphene and other planar sp^2-bonded materials, Phys. Rev. B 80 (2009) 033407, http://dx.doi.org/10.1103/PhysRevB.80.033407.

[41] A.J. Stone, D.J. Wales, Theoretical studies of icosahedral C_{60} and some related species, Chem. Phys. Lett. 128 (1986) 501–503, http://dx.doi.org/10.1016/0009-2614(86)80661-3.

[42] C.P. Ewels, M.I. Heggie, P.R. Briddon, Adatoms and nanoengineering of carbon, Chem. Phys. Lett. 351 (2002) 178–182, http://dx.doi.org/10.1016/S0009-2614(01)01371-9.

[43] H.F. Bettinger, B.I. Yakobson, G.E. Scuseria, Scratching the surface of buckminsterfullerene: The barriers for Stone–Wales transformation through symmetric and asymmetric transition states, J. Am. Chem. Soc. 125 (2003) 5572–5580, http://dx.doi.org/10.1021/ja0288744.

[44] Y. Kumeda, D.J. Wales, Ab initio study of rearrangements between C_{60} fullerenes, Chem. Phys. Lett. 374 (2003) 125–131, http://dx.doi.org/10.1016/S0009-2614(03)00668-7.

[45] W.-W. Wang, J.-S. Dang, J.-J. Zheng, X. Zhao, S. Nagase, Selective growth of fullerenes from C_{60} to C_{70}: Inherent geometrical connectivity hidden in discrete experimental evidence, J. Phys. Chem. C 117 (2013) 2349–2357, http://dx.doi.org/10.1021/jp3100766.

[46] M.-Y. Li, Y.-X. Zhao, Y.-B. Han, K. Yuan, S. Nagase, M. Ehara, X. Zhao, Theoretical investigation of the key roles in fullerene-formation mechanisms: Enantiomer and enthalpy, ACS Appl. Nano Mater. 3 (2020) 547–554, http://dx.doi.org/10.1021/acsanm.9b02110.

[47] M. Endo, H.W. Kroto, Formation of carbon nanofibers, J. Phys. Chem. 96 (1992) 6941–6944, http://dx.doi.org/10.1021/j100196a017.

[48] A.M. Popov, I.V. Lebedeva, S.A. Vyrko, N.A. Poklonski, Multiscale modeling strategy to solve fullerene formation mystery, Fuller. Nanotubes Carbon Nanostruct. 29 (2021) 755–766, http://dx.doi.org/10.1080/1536383X.2021.1900124.

[49] A. Iranmanesh, A.R. Ashrafi, A. Graovac, F. Cataldo, O. Ori, Wiener index role in topological modeling of hexagonal systems – from fullerenes to graphene, in: I. Gutman, B. Furtula (Eds.), Distance in Molecular Graphs – Applications, Univ. Kragujevac, Kragujevac, 2012, pp. 135–155.

[50] D. Vukicevic, F. Cataldo, O. Ori, A. Graovac, Topological efficiency of C_{66} fullerene, Chem. Phys. Lett. 501 (2011) 442–445, http://dx.doi.org/10.1016/j.cplett.2010.11.055.

[51] M.V. Putz, O. Ori, F. Cataldo, A.-M. Putz, Parabolic reactivity "coloring" molecular topology: Application to carcinogenic PAHs, Curr. Org. Chem. 17 (2013) 2816–2830, http://dx.doi.org/10.2174/13852728113179990128.

[52] D. Sabirov, O. Ori, I. László, Isomers of the C_{84} fullerene: A theoretical consideration within energetic, structural, and topological approaches, Fuller. Nanotubes Carbon Nanostruct. 26 (2018) 100–110, http://dx.doi.org/10.1080/1536383X.2017.1405389.

[53] H.W. Kroto, The stability of the fullerenes C_n, with $n = 24$, 28, 32, 36, 50, 60 and 70, Nature 329 (1987) 529–531, http://dx.doi.org/10.1038/329529a0.

[54] M. Yu, I. Chaudhuri, C. Leahy, S.Y. Wu, C.S. Jayanthi, Energetics, relative stabilities, and size-dependent properties of nanosized carbon clusters of different families: Fullerenes, bucky-diamond, icosahedral, and bulk-truncated structures, J. Chem. Phys. 130 (2009) 184708, http://dx.doi.org/10.1063/1.3124827.

[55] J. Kürti, G. Kresse, H. Kuzmany, First-principles calculations of the radial breathing mode of single-wall carbon nanotubes, Phys. Rev. B 58 (1998) R8869–R8872, http://dx.doi.org/10.1103/PhysRevB.58.R8869.

[56] A.I. Siahlo, N.A. Poklonski, A.V. Lebedev, I.V. Lebedeva, A.M. Popov, S.A. Vyrko, A.A. Knizhnik, Y.E. Lozovik, Structure and energetics of carbon, hexagonal boron nitride, and carbon/hexagonal boron nitride single-layer and bilayer nanoscrolls, Phys. Rev. Mater. 2 (2018) 036001, http://dx.doi.org/10.1103/PhysRevMaterials.2.036001.

[57] H. Dai, J.H. Hafner, A.G. Rinzler, D.T. Colbert, R.E. Smalley, Nanotubes as nanoprobes in scanning probe microscopy, Nature 384 (1996) 147–150, http://dx.doi.org/10.1038/384147a0.

[58] S.S. Wong, E. Joselevich, A.T. Woolley, C.L. Cheung, C.M. Lieber, Covalently functionalized nanotubes as nanometre-sized probes in chemistry and biology, Nature 394 (1998) 52–55, http://dx.doi.org/10.1038/27873.

[59] W.A. de Heer, A. Châtelain, D. Ugarte, A carbon nanotube field-emission electron source, Science 270 (1995) 1179–1180, http://dx.doi.org/10.1126/science.270.5239.1179.

[60] P.G. Collins, A. Zettl, A simple and robust electron beam source from carbon nanotubes, Appl. Phys. Lett. 69 (1996) 1969–1971, http://dx.doi.org/10.1063/1.117638.

[61] D.-S. Chung, S.H. Park, H.W. Lee, J.H. Choi, S.N. Cha, J.W. Kim, J.E. Jang, K.W. Min, S.H. Cho, M.J. Yoon, J.S. Lee, C.K. Lee, J.H. Yoo, J.-M. Kim, J.E. Jung, Y.W. Jin, Y.J. Park, J.B. You, Carbon nanotube electron emitters with a gated structure using backside exposure processes, Appl. Phys. Lett. 80 (2002) 4045–4047, http://dx.doi.org/10.1063/1.1480104.

[62] A.V. Krasheninnikov, K. Nordlund, Ion and electron irradiation-induced effects in nanostructured materials, J. Appl. Phys. 107 (2010) 071301, http://dx.doi.org/10.1063/1.3318261.

[63] Y.G. Polynskaya, A.S. Sinitsa, S.A. Vyrko, O. Ori, A.M. Popov, A.A. Knizhnik, N.A. Poklonski, Y.E. Lozovik, Data for: Expansion of nanotube cap due to migration of sp atoms from lateral surface, Mendeley Data, 2022, http://dx.doi.org/10.17632/trgdpzm3gz.